Syntheses and Structures of the New Quaternary Compounds Ba$_4$Nd$_2$Cd$_3$Se$_{10}$ and Ba$_4$*Ln*$_2$Cd$_3$S$_{10}$ (*Ln* = Sm, Gd, Tb)

Yuting Yang and James A. Ibers

Department of Chemistry, Northwestern University, 2145 Sheridan Road, Evanston, Illinois 60208-3113

The compounds Ba$_4$Nd$_2$Cd$_3$Se$_{10}$ and Ba$_4$*Ln*$_2$Cd$_3$S$_{10}$ (*Ln* = Sm, Gd, Tb) have been synthesized at 1173 K with the use of a BaBr$_2$/ KBr eutectic flux. These isostructural compounds crystallize as racemic twins in space group *Cmc*2$_1$ of the orthorhombic system in cells of (*Ln*, *Q*, *a*, *b*, *c* (Å), *T* (K)): Nd, Se, 4.3340(9), 18.667(4), 27.376(6), 115; Sm, S, 4.1907(8), 17.931(4), 26.594(5), 153; Gd, S, 4.1726(4), 17.928(2), 26.638(3), 153; Tb, S, 4.1643(8), 17.916(4), 26.581(5), 153. The corresponding *R*$_1$ indices for the refined structures are 0.053, 0.029, 0.032, and 0.030. The structure comprises [*Ln*$_2$Cd$_3$*Q*$_{10}$]$^{4-}$ layers interconnected by Ba atoms. There are *LnQ*$_6$ octahedra and severely distorted Cd*Q*$_4$ tetrahedra in the structure. Ba$_4$Tb$_2$Cd$_3$S$_{10}$, which is paramagnetic, obeys the Curie–Weiss law and has an effective magnetic moment of 9.94(3) μ_B. A band gap of 3.0 eV for this material was deduced from its diffuse reflectance spectrum. © 2000 Academic Press

INTRODUCTION

Recently, many new quaternary alkaline-earth rare-earth chalcogenides have been synthesized. For *Q* = S, Se these include Ba*LnMQ*$_3$ (*Ln* = rare earth, *M* = Cu, Ag; KZrCuS$_3$ structure type) (1, 2), BaSc$_3$AgS$_6$ (3), Ba$_2$*Ln*Ag$_5$S$_6$ (*Ln* = La and Y) (4), CaLaAl$_3$S$_7$ (5), CaYbInQ$_4$ (Mg$_2$SiO$_4$ structure type) (6), Ca$_4$*Ln*$_2$In$_4$*Q*$_{13}$ (*Ln* = La, Nd, Sm, Gd) (7), and Sr$_3$La$_2$Sn$_3$S$_{12}$ (Eu$_5$Sn$_3$S$_{12}$ structure type, i.e., Eu$^{II}_3$Eu$^{III}_2$Sn$_3$Se$_{12}$) (8). The valence state of the third cation, that is, Cu^I, Ag^I, Al^{III}, In^{III}, or Sn^{IV}, in these alkaline-earth rare-earth chalcogenides has a profound effect on the stoichiometry, and further on the resultant structure type. No structures with this third cation having a valence state of II have been reported. The introduction of Cd^{II}, which is known to be tetrahedrally coordinated in a number of ternary and quaternary alkali- or alkaline-earth compounds (9–14), clearly represents an extension of these studies and leads to new materials, as described here.

EXPERIMENTAL

Syntheses

The compounds Ba$_4$Nd$_2$Cd$_3$Se$_{10}$ and Ba$_4$*Ln*$_2$Cd$_3$S$_{10}$ (*Ln* = Sm, Gd, Tb) were prepared by the reaction of stoichiometric amounts of the rare earth (Alfa Aesar, 99.9%), Cd (Alfa Aesar, 99.999%), *Q* (S, Alfa Aesar, 99.7%; Se, Aldrich, 99.5%), and Ba*Q* (BaS, Alfa Aesar, 99.7%; BaSe, Alfa Aesar, 99.5%) in fused silica tubes with the use of a BaBr$_2$/KBr eutectic flux (molar ratio 1.1/1). The tubes were evacuated, sealed, and then heated in a furnace to 1173 K, where they were kept for 7 days before being cooled at the rate of 3 K/h to 673 K, where the furnace was shut off. The air-stable compounds Ba$_4$*Ln*$_2$Cd$_3$*Q*$_{10}$ are light-brown in color and flat needles in habit. EDX analysis with a Hitachi S4500 scanning electron microscope confirmed the presence of Ba/*Ln*/Cd/*Q* in the approximate ratio 4/2/3/10. The yields of Ba$_4$*Ln*$_2$Cd$_3$*Q*$_{10}$ range from 20 to 60%, depending on the rare earth. Impurities consist of crystals of binary and ternary cadmium compounds, mainly Cd*Q*, Ba$_2$Cd*Q*$_3$, and BaCd*Q*$_2$. For *Q* = Se, only Ba$_4$Nd$_2$Cd$_3$Se$_{10}$ could be obtained in this way.

Crystallography

Diffraction data from a single crystal of Ba$_4$Nd$_2$Cd$_3$Se$_{10}$ were collected at 115 K on a Picker automatic four-circle diffractometer (15). Thirty peaks in the 2θ range 30–35° were used to obtain the unit cell. Data from all the other compounds in the series were collected at 153 K on a Bruker SMART-1000 CCD diffractometer (16) at 15 or 25 s for each frame and with a step of 0.25° or 0.3° in ω. Face-indexed absorption corrections were applied to all data sets. The data collected on the CCD diffractometer were further corrected for frame variations with the use of the program SADABS (16). Systematic absences and Laue symmetry led to the orthorhombic space groups *Cmc*2$_1$ or *Cmcm*. In each instance no solution could be found in space group *Cmcm*, but a solution was found in space group *Cmc*2$_1$ with the use of the direct methods program SHELXS (17). Each

384

TABLE 1
Crystal Data and Structure Refinement for Ba$_4$Ln$_2$Cd$_3$Q$_{10}$

	Ba$_4$Nd$_2$Cd$_3$Se$_{10}$	Ba$_4$Sm$_2$Cd$_3$S$_{10}$	Ba$_4$Gd$_2$Cd$_3$S$_{10}$	Ba$_4$Cd$_3$Tb$_2$S$_{10}$
Formula weight	1964.64	1507.86	1521.66	1525.00
a (Å)	4.3340(9)	4.1907(8)	4.1726(4)	4.1643(8)
b (Å)	18.667(4)	17.931(4)	17.928(2)	17.916(4)
c (Å)	27.376(6)	26.594(5)	26.638(3)	26.581(5)
Space group	$Cmc2_1$	$Cmc2_1$	$Cmc2_1$	$Cmc2_1$
Z	4	4	4	4
T (K)	115	153	153	153
Volume	2214.9(8)	1998.3(7)	1992.7(3)	1983.2(7)
λ (Å)	0.71073	0.71073	0.71073	0.71073
ρ_c (g/cm^3)	5.892	5.012	5.072	5.108
μ (cm^{-1})	308.2	176.7	184.8	190.1
Transmission factors	0.27–0.39	0.22–0.71	0.25–0.77	0.23–0.64
Reflections collected/unique	10570/3045	8824/2689	6344/2563	6307/1943
$R1^a$ ($F_o^2 > 2\sigma(F_o^2)$)	0.0532	0.0288	0.0315	0.0302
wR_2^b (all data)	0.104	0.0678	0.0708	0.0699

$^a R_1 = \sum \|F_o| - |F_c\| / \sum |F_o|; F_o^2 > 2\sigma(F_o^2)$.
$^b wR_2 = \{\sum[w(F_o^2 - F_c^2)^2]/\sum wF_o^4\}^{1/2}; w^{-1} = \sigma^2(F_o^2) + (0.04 \times F_o^2)^2$ for $F_o^2 \geq 0$ and $w^{-1} = \sigma^2(F_o^2)$ for $F_o^2 < 0$.

structure was refined by full-matrix least-squares methods with the program SHELXL in the SHELXTL-97 suite (17). In each refinement the Flack parameter was near 0.5, suggesting either a racemic twin or the possibility that the true space group is $Cmcm$. However, examination of the resultant atomic coordinates with the program MISSYM (18) indicates that the positions of atoms Cd3 and S6 are inconsistent with the additional symmetry of space group $Cmcm$.

The improvement in R indices on refinement of these structures as racemic twins is slight but significant. In no instance was the residual electron density greater than 10% of the height of a chalcogen atom in the given structure. The refined cell parameters and other relevant crystal data are given in Table 1, and the final atomic parameters and equivalent isotropic displacement parameters are given in Table 2.

TABLE 2
Atomic Coordinates^a and Equivalent Isotropic Displacement Parameters (Å^2) for Ba$_4$Ln$_2$Cd$_3$Q$_{10}$

	Ba$_4$Nd$_2$Cd$_3$Se$_{10}$			Ba$_4$Sm$_2$Cd$_3$S$_{10}$			Ba$_4$Gd$_2$Cd$_3$S$_{10}$			Ba$_4$Tb$_2$Cd$_3$S$_{10}$		
Atom	y	z	U^b	y	z	U	y	z	U	y	z	U
Ln(1)	0.08348(7)	0.74614(10)	0.0072(3)	0.08022(3)	0.74627(3)	0.00968(14)	0.07966(4)	0.74642(4)	0.00976(15)	0.07939(4)	0.74652(5)	0.00937(16)
Ln(2)	0.50272(11)	0.00004(11)	0.0048(3)	0.50320(4)	0.00000(3)	0.01007(14)	0.50342(5)	0.00000(4)	0.01017(15)	0.50334(5)	0.00000(5)	0.00967(17)
Ba(1)	0.16470(10)	0.60647(8)	0.0065(4)	0.16111(4)	0.60796(3)	0.00964(18)	0.16029(5)	0.60816(4)	0.0096(2)	0.16006(5)	0.60859(4)	0.0086(2)
Ba(2)	0.16603(11)	0.89104(8)	0.0067(4)	0.16300(4)	0.89006(3)	0.00947(17)	0.16253(5)	0.88976(4)	0.0094(2)	0.16231(5)	0.88953(4)	0.0090(2)
Ba(3)	0.57691(10)	0.34162(8)	0.0071(5)	0.57706(4)	0.34362(3)	0.01092(19)	0.57686(5)	0.34350(4)	0.0113(2)	0.57686(6)	0.34377(5)	0.0107(2)
Ba(4)	0.59364(10)	0.16019(8)	0.0072(4)	0.59663(5)	0.16102(3)	0.01300(19)	0.59673(5)	0.16089(4)	0.0133(2)	0.59634(6)	0.16079(5)	0.0129(2)
Cd(1)	0.15067(13)	0.45475(10)	0.0070(5)	0.15719(6)	0.45605(4)	0.0125(2)	0.15702(7)	0.45617(5)	0.0124(3)	0.15706(7)	0.45641(6)	0.0119(3)
Cd(2)	0.15763(13)	0.03910(9)	0.0058(5)	0.16273(6)	0.03843(4)	0.0119(2)	0.16269(7)	0.03846(5)	0.0122(3)	0.16236(7)	0.03851(6)	0.0115(3)
Cd(3)	0.21640(13)	0.26799(9)	0.0142(5)	0.21981(6)	0.26852(4)	0.0152(2)	0.21978(7)	0.26861(4)	0.0151(3)	0.21962(7)	0.26836(5)	0.0147(3)
Q(1)	0.01024(18)	0.42571(14)	0.0046(8)	0.0126(2)	0.42758(14)	0.0091(7)	0.0122(2)	0.42818(18)	0.0111(9)	0.0124(2)	0.4286(2)	0.0093(10)
Q(2)	0.01546(17)	0.07080(15)	0.0033(8)	0.0172(2)	0.06858(14)	0.0094(7)	0.0171(2)	0.06805(16)	0.0077(9)	0.0165(3)	0.06769(19)	0.0091(10)
Q(3)	0.07179(13)	0.25162(18)	0.0071(6)	0.07441(16)	0.25249(18)	0.0100(6)	0.07429(18)	0.2529(2)	0.0080(7)	0.07395(19)	0.2527(2)	0.0086(8)
Q(4)	0.20701(18)	0.36884(14)	0.0062(7)	0.2079(2)	0.36859(15)	0.0119(6)	0.2078(2)	0.36842(18)	0.0124(8)	0.2075(2)	0.3687(2)	0.0117(9)
Q(5)	0.21077(17)	0.12469(13)	0.0058(7)	0.21360(19)	0.12316(12)	0.0083(6)	0.2141(2)	0.12300(14)	0.0074(8)	0.2142(2)	0.12301(17)	0.0071(9)
Q(6)	0.23894(16)	0.72970(11)	0.0106(6)	0.23514(19)	0.73146(14)	0.0136(7)	0.2335(2)	0.73207(15)	0.0126(8)	0.2332(2)	0.7322(2)	0.0153(10)
Q(7)	0.34105(17)	0.48315(13)	0.0057(8)	0.34142(19)	0.48264(15)	0.0111(8)	0.3422(2)	0.48248(17)	0.0120(10)	0.3429(2)	0.4826(2)	0.0106(11)
Q(8)	0.34465(17)	0.01003(14)	0.0061(8)	0.34654(18)	0.01030(15)	0.0099(7)	0.3478(2)	0.01090(17)	0.0085(9)	0.3489(2)	0.0111(2)	0.0093(10)
Q(9)	0.40708(19)	0.31893(15)	0.0100(8)	0.40936(18)	0.31692(15)	0.0092(7)	0.4096(2)	0.31610(17)	0.0095(9)	0.4101(2)	0.3157(2)	0.0094(10)
Q(10)	0.41950(17)	0.17506(13)	0.0066(8)	0.42342(19)	0.17716(15)	0.0100(7)	0.4238(2)	0.17761(17)	0.0091(9)	0.4240(2)	0.1783(2)	0.0083(9)

^{a}All atoms are in position 0, y, z in space group $Cmc2_1$.
$^b U$ is the equivalent isotropic displacement parameter and is defined as one-third of the trace of the orthogonalized U_{ij} tensor.
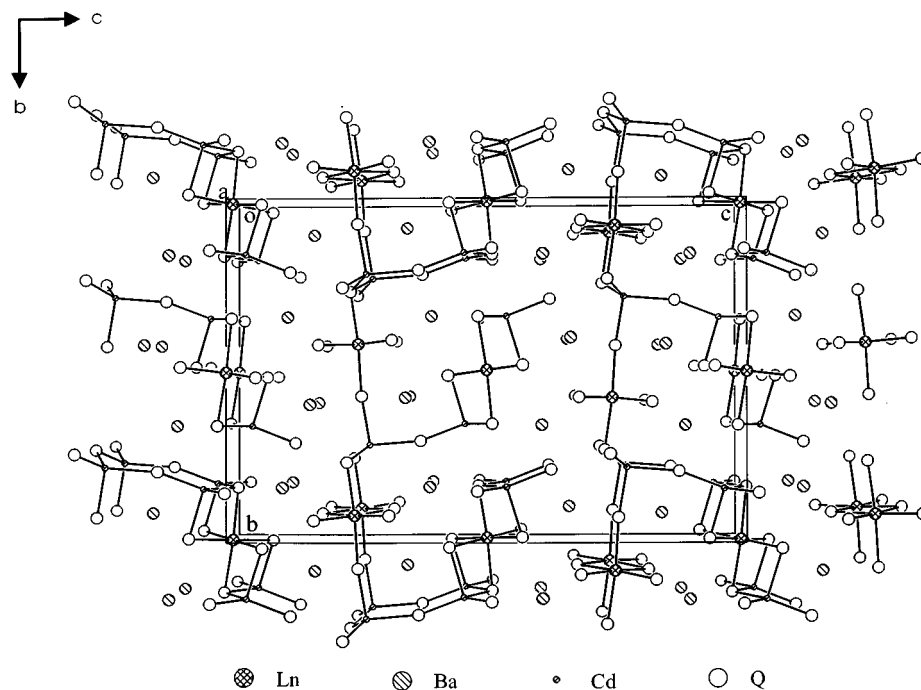
FIG. 1. Structure of $Ba_4Ln_2Cd_3Q_{10}$.

Magnetic Susceptibility

As the compound can be obtained in high yield, single crystals of $Ba_4Tb_2Cd_3S_{10}$ were picked out and ground. The magnetic susceptibility measurements on this compound were made at 50 G over the temperature range 2–300 K with a zero field cooling with a Quantum Design SQUID magnetometer. No measurements were made at high field. Data were corrected for the diamagnetic contributions of the atomic cores (19).
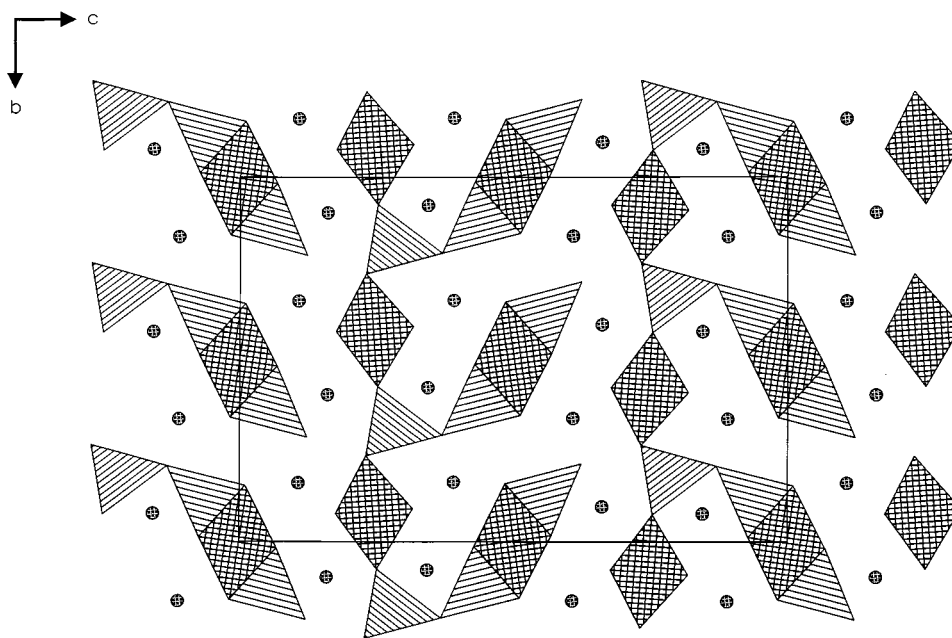

FIG. 2. Polyhedral view of $Ba_4Ln_2Cd_3Q_{10}$.

UV-Vis Diffuse Reflectance Spectroscopy

A Cary 1E UV-visible spectrophotometer with a diffuse reflectance accessory was used to measure the diffuse reflectance spectrum over the range 350 to 900 nm at 293 K on the compound $Ba_4Tb_2Cd_3S_{10}$. A Varian Halon plate was used as a reference.

RESULTS

The structure of $Ba_4Ln_2Cd_3Q_{10}$, which is a new structure type, is shown in Fig. 1; Fig. 2 is a polyhedral representation of the structure. The structure comprises $[Ln_2Cd_3Q_{10}]^{4-}$ layers interconnected by Ba atoms. An infinite main plane perpendicular to c consists of chains of edge-shared LnQ_6 octahedra and corner-shared CdQ_4 tetrahedra that share corners with one another along b. Branching planes composed of CdQ_4–LnQ_6–CdQ_4 units at the corners of the CdQ_4 tetrahedra stick out along c from the main plane up and down along b for two consecutive main planes. These CdQ_4 tetrahedra are severely distorted, which is not uncommon in the chalcogenides (e.g., $Na_4Cd_3Se_5$ (10), $K_2Cd_3S_4$ (13), $Na_6Cd_7S_{10}$ (14)).

There are four crystallographically independent Ba atoms in the structure: Ba2 and Ba3 are coordinated by seven Q atoms in a monocapped trigonal prism, whereas Ba1 and Ba4 are coordinated by eight Q atoms in a bicapped trigonal prism.

The bond lengths and angles given in Tables 3 and 4 are normal. For example, compare the Cd–S bond lengths of 2.430(5) to 2.729(4) Å with those of 2.47(1) to 2.67(1) Å in $Rb_2Cd_3S_4$ (13), the Cd–Se bond lengths of 2.544(4) to 2.792(4) Å with those of 2.593(3) to 2.780(2) Å in $Rb_2Cd_3Se_4$ (13), the Sm–S bond lengths of 2.777(3) to 2.860(3) Å with

TABLE 3
Bond Lengths (Å) for $Ba_4Ln_2Cd_3Q_{10}$

Bond lengths	$Ba_4Nd_2Cd_3Se_{10}$	$Ba_4Sm_2Cd_3S_{10}$	$Ba_4Gd_2Cd_3S_{10}$	$Ba_4Tb_2Cd_3S_{10}$
$Ln(1)$–$Q(3)$	2.902(3)	2.777(3)	2.765(3)	2.752(4)
$Ln(1)$–$Q(10) \times 2$	2.913(3)	2.788(3)	2.778(3)	2.762(4)
$Ln(1)$–$Q(6)$	2.937(3)	2.806(3)	2.784(4)	2.781(4)
$Ln(1)$–$Q(9) \times 2$	2.949(3)	2.820(3)	2.799(3)	2.784(4)
$Ln(2)$–$Q(2) \times 2$	2.916(3)	2.789(3)	2.775(3)	2.762(4)
$Ln(2)$–$Q(7)$	2.953(4)	2.824(4)	2.806(4)	2.793(5)
$Ln(2)$–$Q(8)$	2.963(4)	2.822(3)	2.806(4)	2.783(4)
$Ln(2)$–$Q(1) \times 2$	2.982(3)	2.860(3)	2.844(3)	2.831(4)
Ba(1)–$Q(5) \times 2$	3.217(3)	3.098(3)	3.095(3)	3.092(3)
Ba(1)–$Q(10) \times 2$	3.270(3)	3.174(3)	3.169(3)	3.168(4)
Ba(1)–$Q(8) \times 2$	3.420(4)	3.340(3)	3.330(4)	3.329(5)
Ba(1)–$Q(2)$	3.502(4)	3.365(4)	3.356(4)	3.345(5)
Ba(1)–$Q(6)$	3.647(4)	3.542(4)	3.552(4)	3.538(5)
Ba(2)–$Q(9) \times 2$	3.234(3)	3.140(3)	3.142(3)	3.142(4)
Ba(2)–$Q(4) \times 2$	3.268(3)	3.174(3)	3.175(3)	3.175(3)
Ba(2)–$Q(7) \times 2$	3.327(3)	3.234(3)	3.234(4)	3.235(4)
Ba(2)–$Q(1)$	3.425(4)	3.303(4)	3.296(4)	3.297(5)
Ba(3)–$Q(9)$	3.230(4)	3.088(3)	3.087(4)	3.079(4)
Ba(3)–$Q(3) \times 2$	3.283(4)	3.197(4)	3.190(4)	3.193(5)
Ba(3)–$Q(4) \times 2$	3.339(3)	3.217(3)	3.210(3)	3.202(3)
Ba(3)–$Q(1) \times 2$	3.398(4)	3.279(3)	3.284(4)	3.280(4)
Ba(4)–$Q(5) \times 2$	3.228(3)	3.131(3)	3.131(3)	3.131(3)
Ba(4)–$Q(10)$	3.276(4)	3.135(3)	3.133(4)	3.123(4)
Ba(4)–$Q(3) \times 2$	3.336(4)	3.235(4)	3.245(4)	3.235(5)
Ba(4)–$Q(2) \times 2$	3.580(4)	3.530(3)	3.536(4)	3.536(4)
Ba(4)–$Q(6)$	3.659(4)	3.551(4)	3.586(4)	3.597(5)
Cd(1)–$Q(4)$	2.576(5)	2.498(4)	2.509(5)	2.501(6)
Cd(1)–$Q(8) \times 2$	2.645(3)	2.545(2)	2.547(3)	2.541(3)
Cd(1)–$Q(1)$	2.739(4)	2.700(4)	2.701(4)	2.696(5)
Cd(2)–$Q(5)$	2.544(4)	2.431(3)	2.434(4)	2.430(5)
Cd(2)–$Q(7) \times 2$	2.654(2)	2.569(2)	2.566(3)	2.560(3)
Cd(2)–$Q(2)$	2.792(4)	2.729(4)	2.726(4)	2.726(5)
Cd(3)–$Q(6) \times 2$	2.548(2)	2.452(2)	2.450(2)	2.444(3)
Cd(3)–$Q(3)$	2.736(3)	2.642(3)	2.642(4)	2.643(4)
Cd(3)–$Q(4)$	2.767(5)	2.670(4)	2.667(5)	2.675(6)

TABLE 4
Bond Angles (°) for Ba$_4$Ln$_2$Cd$_3$Q$_{10}$

Bond Angles	Ba$_4$Nd$_2$Cd$_3$Se$_{10}$	Ba$_4$Sm$_2$Cd$_3$S$_{10}$	Ba$_4$Gd$_2$Cd$_3$S$_{10}$	Ba$_4$Tb$_2$Cd$_3$S$_{10}$
$Q(3)$–$Ln(1)$–$Q(10) \times 2$	90.89(10)	90.91(10)	91.11(11)	90.99(13)
$Q(10)$–$Ln(1)$–$Q(10)$	96.13(13)	97.45(12)	97.36(14)	97.86(17)
$Q(3)$–$Ln(1)$–$Q(6)$	174.15(15)	175.34(13)	175.71(15)	175.57(18)
$Q(10)$–$Ln(1)$–$Q(6) \times 2$	85.21(9)	86.02(9)	86.06(11)	86.10(12)
$Q(3)$–$Ln(1)$–$Q(9) \times 2$	91.42(10)	91.52(9)	91.56(11)	91.61(12)
$Q(10)$–$Ln(1)$–$Q(9) \times 2$	177.57(10)	177.46(10)	177.28(12)	177.35(13)
$Q(10)$–$Ln(1)$–$Q(9) \times 2$	84.60(5)	83.24(7)	83.07(7)	82.61(9)
$Q(6)$–$Ln(1)$–$Q(9) \times 2$	92.55(9)	91.60(8)	91.30(9)	91.33(11)
$Q(9)$–$Ln(1)$–$Q(9)$	94.58(14)	95.96(12)	96.38(14)	96.80(17)
$Q(2)$–$Ln(2)$–$Q(2)$	95.99(15)	97.39(12)	97.51(14)	97.85(17)
$Q(2)$–$Ln(2)$–$Q(7) \times 2$	91.35(9)	91.02(9)	91.22(10)	91.34(12)
$Q(2)$–$Ln(2)$–$Q(8) \times 2$	91.14(10)	91.51(9)	91.18(10)	90.93(12)
$Q(7)$–$Ln(2)$–$Q(8)$	176.29(17)	176.17(14)	176.37(16)	176.54(19)
$Q(2)$–$Ln(2)$–$Q(1) \times 2$	178.60(14)	178.38(10)	178.37(13)	178.30(15)
$Q(2)$–$Ln(2)$–$Q(1) \times 2$	85.41(5)	84.20(6)	84.07(7)	83.72(8)
$Q(7)$–$Ln(2)$–$Q(1) \times 2$	88.47(10)	89.30(9)	89.16(10)	89.27(12)
$Q(8)$–$Ln(2)$–$Q(1) \times 2$	88.98(10)	88.09(9)	88.38(11)	88.39(12)
$Q(1)$–$Ln(2)$–$Q(1)$	93.20(14)	94.21(11)	94.36(15)	94.69(16)
$Q(4)$–Cd(1)–$Q(8) \times 2$	120.59(9)	122.52(8)	123.06(9)	123.24(11)
$Q(8)$–Cd(1)–$Q(8)$	110.05(16)	110.84(15)	110.02(17)	110.1(2)
$Q(4)$–Cd(1)–$Q(1)$	97.22(14)	95.09(12)	95.26(14)	95.28(16)
$Q(8)$–Cd(1)–$Q(1) \times 2$	101.40(10)	97.69(9)	97.22(11)	96.68(12)
$Q(5)$–Cd(2)–$Q(7) \times 2$	121.86(8)	123.11(7)	123.42(9)	123.40(10)
$Q(7)$–Cd(2)–$Q(7)$	109.48(15)	109.33(14)	108.80(16)	108.9(2)
$Q(5)$–Cd(2)–$Q(2)$	94.84(15)	94.95(12)	95.47(14)	95.93(15)
$Q(7)$–Cd(2)–$Q(2) \times 2$	100.85(11)	98.16(9)	97.77(11)	97.46(12)
$Q(6)$–Cd(3)–$Q(6)$	116.56(16)	117.39(15)	116.76(16)	116.86(19)
$Q(6)$–Cd(3)–$Q(3) \times 2$	104.81(10)	105.08(10)	105.96(11)	106.25(12)
$Q(6)$–Cd(3)–$Q(4) \times 2$	115.55(8)	115.27(9)	115.06(10)	114.81(12)
$Q(3)$–Cd(3)–$Q(4)$	95.79(14)	94.72(13)	94.48(15)	94.42(17)

FIG. 3. Bond lengths of Ln–S (Å) (Ln = Sm, Gd, Tb) versus ionic radii of Ln^{3+} (Å). $Ln(1)$–S(3) (■); $Ln(1)$–S(10) (◆); $Ln(2)$–S(2) (●); $Ln(1)$–S(6) (▲); $Ln(1)$–S(9) (▼); $Ln(2)$–S(8) (×); $Ln(2)$–S(7) (+); $Ln(2)$–S(1) (∗).
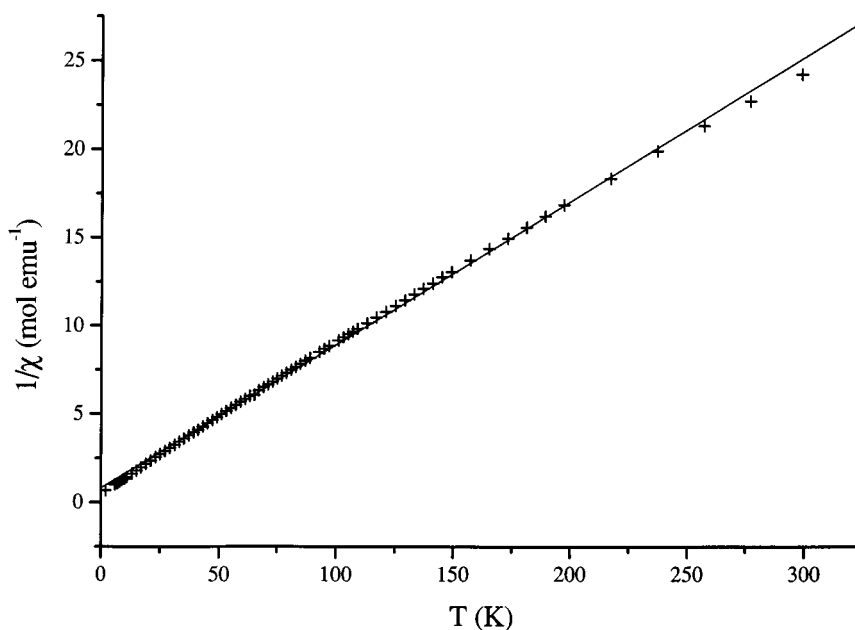
FIG. 4. Reciprocal magnetic susceptibility of $Ba_4Tb_2Cd_3Q_{10}$ vs temperature. The solid line is the fit of the data to the Curie–Weiss law.

those of 2.752(3) to 2.859(3) Å in $Ba_{0.914}Sm_2S_{3.9}$ (20), the Gd–S bond lengths of 2.765(3) to 2.844(3) Å with those of 2.806(4) in $CsGdS_2$ (21), and the Tb–S bond lengths of 2.752(4) to 2.831(4) Å with those of 2.789(9) Å in $CsTbS_2$ (21). A plot (Fig. 3) of Ln–S bond lengths in $Ba_4Ln_2Cd_3S_{10}$ (Ln = Sm, Gd, Tb) versus the Ln^{3+} ionic radius (22) shows the expected trend. As expected, the unit cell volumes in-

crease with increasing size of Ln; however, not all the individual cell constants follow this trend, presumably because of the alignment of the various coordination polyhedra in different directions.

The reciprocal molar magnetic susceptibility (χ^{-1}) of $Ba_4Tb_2Cd_3S_{10}$, shown in Fig. 4, has been fit to the Curie–Weiss law $\chi = C/(T + \theta)$, with parameters $C =$
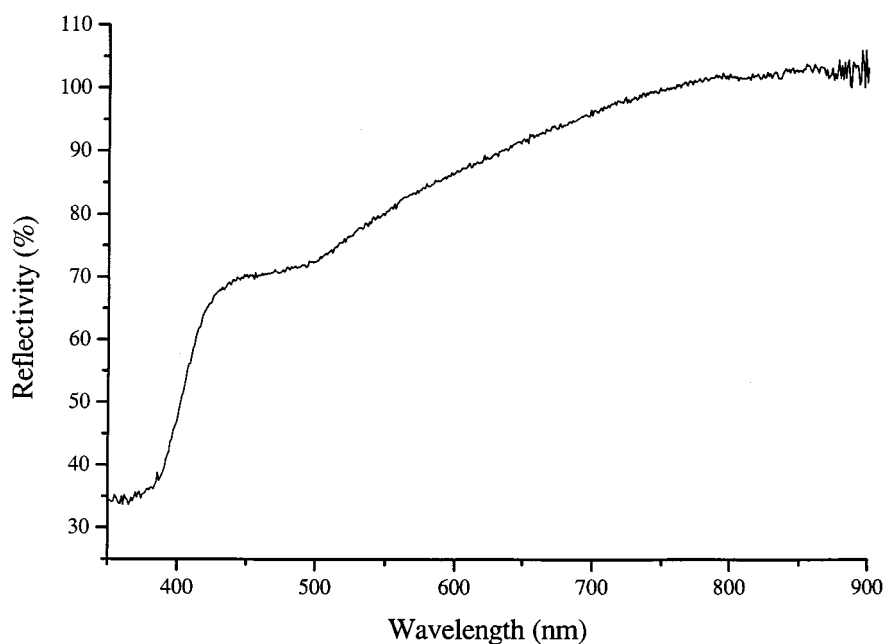

FIG. 5. Diffuse reflectance spectrum of $Ba_4Ln_2Cd_3Q_{10}$.

12.35(6) emu K/mol and $\theta = 9.9(6)$ K. The calculated effective magnetic moment 9.94(3) μ_B may be compared with the theoretical value 9.72 μ_B (23) and the recently published experimental value 9.79 μ_B (24) and 9.25(4) μ_B (25).

The diffuse reflectance spectrum of $Ba_4Tb_2Cd_3S_{10}$ from 350 to 900 nm is shown in Fig. 5. An optical band gap of 3.0 eV was deduced with the use of a straightforward extrapolation method (26). This gap is consistent with the brown color of the material. Because of the limited quantities of material available, no diffuse reflectance spectra were obtained on $Ba_4Nd_2Cd_3Se_{10}$, $Ba_4Sm_2Cd_3S_{10}$, or $Ba_4Gd_2Cd_3S_{10}$. However, they exhibit the same brown color and presumably have similar band gaps.

ACKNOWLEDGMENTS

REFERENCES

1. A. E. Christuk, P. Wu, and J. A. Ibers, *J. Solid State Chem.* **110,** 330 (1994).
2. P. Wu, A. E. Christuk, and J. A. Ibers, *J. Solid State Chem.* **110,** 337 (1994).
3. P. Wu, M. A. Pell, J. A. Cody, and J. A. Ibers, *J. Alloys Compd.* **224,** 199 (1995).
4. P. Wu and J. A. Ibers, *Z. Kristallogr.* **208,** 35 (1993).
5. A.-M. Lozac'h, M. Guittard, and J. Flahaut, *C. R. Séances Acad. Sci. Ser. C* **275,** 809 (1972).
6. J. D. Carpenter and S.-J. Hwu, *Chem. Mater.* **4,** 1368 (1992).
7. J. D. Carpenter and S.-J. Hwu, *Inorg. Chem.* **34,** 4647 (1995).
8. S. Jaulmes and M. Julien-Pouzol, *Acta Crystallogr. Sect. B Struct. Crystallogr. Cryst. Chem.* **33,** 1191 (1977).
9. J. E. Iglesias, K. E. Pachali, and H. Steinfink, *J. Solid State Chem.* **9,** 6 (1974).
10. M. A. Ansari and J. A. Ibers, *J. Solid State Chem.* **103,** 293 (1993).
11. E. A. Axtell III, J.-H. Liao, Z. Pikramenou, Y. Park, and M. G. Kanatzidis, *J. Am. Chem. Soc.* **115,** 12191 (1993).
12. E. A. Axtell III and M. G. Kanatzidis, *Chem. Eur. J.* **4,** 2435 (1998).
13. E. A. Axtell III, J.-H. Liao, Z. Pikramenou, and M. G. Kanatzidis, *Chem. Eur. J.* **2,** 656 (1996).
14. E. A. Axtell III and M. G. Kanatzidis, *Chem. Mater.* **8,** 1350 (1996).
15. J. C. Huffman and W. E. Streib, unpublished work, 1990.
16. SMART Version 5.054 and SAINT-Plus Version 6.0, Data Collection and Processing Software for the SMART System, Bruker Analytical X-Ray Instruments, Madison, WI, 1997, 1999.
17. G. M. Sheldrick, SHELXTL DOS/Windows/NT Version 5.10, Bruker Analytical X-Ray Instruments, Madison, WI, 1997.
18. Y. Le Page, *J. Appl. Crystallogr.* **20,** 264 (1987).
19. L. N. Mulay and E. A. Boudreaux, Eds.,"Theory and Applications of Molecular Diamagnetism." Wiley-Interscience, New York, 1976.
20. J. D. Carpenter and S.-J. Hwu, *Acta Crystallogr. Sect. C Cryst. Struct. Commun.* **48,** 1164 (1992).
21. W. Bronger, W. Brüggemann, M. von der Ahe, and D. Schmitz, *J. Alloys Compd.* **200,** 205 (1993).
22. R. D. Shannon, *Acta Crystallogr. Sect. A Cryst. Phys. Diffr. Theor. Gen. Crystallogr.* **32,** 751 (1976).
23. C. Kittel, "Introduction to Solid State Physics," 6th ed. Wiley, New York, 1986.
24. H. Sen, D. Neogy, and B. M. Wanklyn, *J. Magn. Magn. Mater.* **73,** 221 (1988).
25. A. C. Sutorik and M. G. Kanatzidis, *Chem. Mater.* **9,** 387 (1997).
26. O. Schevciw and W. B. White, *Mater. Res. Bull.* **18,** 1059 (1983).